JOURNAL OF SOLID STATE CHEMISTRY **137,** 346–352 (1998)
ARTICLE NO. SC987747

Modeling the Thermal Decomposition of Solids on the Basis of Lattice Energy Changes

Part 2: Alkaline–Earth Peroxides

Annemarie de La Croix, Robin B. English,† and Michael E. Brown[1]

Chemistry Department, Rhodes University, Grahamstown, 6140 South Africa
E-mail: chmb@warthog.ru.ac.za

and

Leslie Glasser

Centre for Molecular Design, Chemistry Department, University of the Witwatersrand, P O Wits, 2050 South Africa
E-mail: glasser@aurum.chem.wits.ac.za

Received July 22, 1997; in revised form December 21, 1997; accepted December 30, 1997

In Part 1, the decompositions of the alkaline–earth metal (Ca, Sr, Ba) carbonates to their oxides, with the release of CO_2 gas, were modeled by devising a symmetry-based sequence of steps by which the reactant structure is converted to the product structure. Lattice energies were evaluated at each step to yield energy profiles for the postulated reaction processes. The observed (apparent) activation energies were comparable to the energy barriers for the postulated mechanisms, suggesting that the postulated mechanisms are energetically feasible. The calculations are repeated here (in Part 2) for the decompositions of the corresponding alkaline–earth peroxides. The energy barriers found are low compared to the observed activation energies. This result is taken to suggest that the postulated processes are energetically inaccessible. © 1998 Academic Press

INTRODUCTION

In Part 1 of this pair of papers (1) the thermal decompositions of a group of alkaline–earth carbonates (Ca, Sr, Ba) to their corresponding oxides were modeled by setting up a hypothetical symmetry-based pathway of idealized intermediate crystal structures. A profile of lattice energies (corrected for gas evolution) through this sequence was thus established, and compared with the experimentally observed activation energies of the respective thermal decompositions. There proved to be a reasonable correspondence between the measured activation energies and those yielded by the corresponding lattice energy profiles. This result does not, in any way, purport to suggest that the chosen pathway represents the actual mechanism of the decomposition (which, in any case, is likely to be mediated by defects of various kinds). Rather, the experimental activation energy is to be regarded as an *apparent* value, averaged over the many microscopic events occurring during the decomposition; the calculated, symmetry-based lattice energy profile is simply one representation of that decomposition. Its success, or otherwise, as a representation must be judged on the quality of the insights to which this representation leads.

In this paper (Part 2) similar modeling of the decompositions of the corresponding alkaline–earth peroxides to their respective oxides is presented. This study provides an opportunity to examine, by an equivalent method, the effects of the same set of cations in a different structural context, but leading to the same oxide products. The very different results for the peroxide decompositions reported below, compared to results found for the carbonates, provide a measure of the utility of the method in suggesting mechanistic differences between the two types of decompositions.

The reactions examined in Part 2 are represented by:

$$MO_2(s) \rightarrow MO(s) + \tfrac{1}{2}O_2(g).$$

Reactions of this type have been thoroughly studied, as represented by the decompositions (2) of BaO_2 and of SrO_2.

† Deceased.
[1] To whom correspondence should be addressed.

0022-4596/98 $25.00

LATTICE ENERGY CALCULATIONS

The calculations are generally analogous to those described (1) more fully in Part 1. The potential model ("force field") used in this work consists of a sum of Coulombic and exp-6 interaction terms. A, C, and ρ are potential parameters which need to be optimized so that the force field gives the closest representation possible of the known crystal structures when the ion positions and the lattice constants are relaxed (i.e., not constrained during an optimization of the crystal structures). For this treatment, the peroxide ion, O^-–O^-, was chosen as a rigid entity with fixed ion charges and bond length.

The FORTRAN program WMIN (1) by Busing (3) was used to optimize the short-range potentials and perform the energy calculations and optimizations.

STRUCTURAL INFORMATION

The Alkaline–Earth Metal Oxides

The accuracy of lattice energy calculations depends on the quality of the crystal data used as reference. The crystal structures of MgO, CaO, SrO, and BaO belong to the face-centered cubic system. Crystal data are given in Table 1 of Part 1 (1). For ready comparison of the peroxide and oxide structures, an alternative unit cell for the oxides was constructed. A body-centered tetragonal unit cell of half the volume ($Z = 2$) was generated by rotating the x- and y-axes through 45° about the z-axis. The dimensions of the unit cells are related by dividing the lattice constants, a and b, of the cubic face-centered unit cell by a factor of $\sqrt{2}$ to obtain the values for the tetragonal body-centered lattice. The dimension c is the same for both cells, since the body-centered unit cell was derived by rotation about the z-axis.

The Alkaline–Earth Metal Peroxides

The crystal structures of CaO_2, SrO_2, and BaO_2 belong to the body-centered, tetragonal system (CaC_2-type), space group 139, $I4/mmm$, with $Z = 2$ (Table 1). The structure (4) of BaO_2 is reliable and gives a peroxide bond length of 1.49 Å. However, the data (5, 6) for CaO_2 and for SrO_2 are known to be poor (4), possibly due to partial decomposition of the peroxide ion (7), yielding excessively short peroxide bond lengths (1.30 Å). Consequently, the data used for CaO_2 and SrO_2 were constructed from the latest-reported lattice constants, with the O^-–O^- separation adjusted symmetrically about the bond centers to 1.49 Å. The SrO_2 and BaO_2 lattice parameters (4, 8) appear to be reliable since the respective experimental densities (9, 10) are low, but fall within a 5% deviation range. The large deviation for CaO_2, however, indicates inaccuracies in either the lattice constants of CaO_2 or the experimental density, D_o.

Oxides

The optimization of the potential parameters for the oxides is reported (1) in full in Part 1. The same set of optimized oxide parameters (OPT2) was used in both studies (see Part 1, Table 3).

Peroxides

The optimization of the potential parameters for Sr and Ba peroxides was done with reference to the crystal structures with O–O = 1.49 Å; the CaO_2 parameters were omitted because the accuracy of the crystal data reported for CaO_2 is questionable. All symmetry constraints were removed, allowing all six cell dimensions to be used as observables. (As noted in Part 1, this does not provide a set of six independent lattice constants, but provides a feasible solution to the least-squares problem.) For starting values, the oxide parameter set, OPT2, and a "mixed oxide–peroxide" structure—constructed by substituting an oxide for the peroxide, so that the oxygen would be in the same oxidation state as in the oxide, but otherwise retaining the space group and lattice dimensions of the peroxide structures—were used. This approach failed, probably due to the hypothetical structures being too unstable. Starting values were then selected on a trial-and-error basis by combining oxide and

TABLE 1
Crystal Data for the Alkaline–Earth Metal Peroxides (Tetragonal space group No. 139, *I4/mmm*, with $Z = 2$, with O–O set to 1.49 Å)

		Lattice constants			Unit cell volume	Experimental density	Density ratio
	(Ref.)	a (Å)	c (Å)	c/a	V (Å^3)	D_0 (g cm^{-3})	(expt/calc)
CaO_2	(5)	3.54	5.92	1.67	74.19	2.92 (9)	0.907
SrO_2	(8)	3.568	6.616	1.85	84.23	4.56 (9)	0.965
BaO_2	(4)	3.807	6.841	1.80	99.15	5.43 (10)	0.958

TABLE 2
Optimized Short-Range Parameters (A_{ij}, ρ_{ij}, and C_{ij}) for each Ion Pair Combination in the Alkaline–Earth Metal Peroxides

Parameters	OPT9 (O–O = 1.49 Å)
A_{ij} (kJ mol^{-1})	
O–O	35.86485×10^8
Sr–O	7.31160×10^4
Ba–O	1.70120×10^4
ρ_{ij} (Å)	
O–O	0.1546
Sr–O	0.3751
Ba–O	0.5152
C_{ij} (kJ mol^{-1} Å^6)	
O–O	338.9678×10^2
RDWST[a]	0.183×10^{-3}

[a] RDWST is the square root of the sum, over all the substances, of the derivatives of the lattice energy with respect to each parameter, plus the squares of the differences between the observed and calculated data (1).

carbonate parameters, and yielded the optimized set OPT9 (the numbering of parameter sets continues from those sets used in Part 1) (Table 2).

The optimized parameter set, OPT9, was then used to calculate the lattice energies of the peroxides (Table 3). The relaxed structures of both SrO_2 and BaO_2 are very close to their respective experimental structures (errors of 0.5%), and the calculated lattice energies are adequately close to the range of reported values (11–14) (Table 4).

MODELING THE THERMAL DECOMPOSITION OF ALKALINE–EARTH METAL PEROXIDES TO OXIDES

To investigate the changes in lattice energy during the thermal decomposition of alkaline–earth metal peroxides to their respective solid oxides and gaseous O_2, i.e.,

$$MO_2(s) \rightarrow MO(s) + \tfrac{1}{2}O_2(g),$$

symmetry-controlled routes for transforming the reactant structure into the solid product structure were devised.

TABLE 3
Cell Dimensions (a, c), Volumes (V), and Lattice Energies (W) Calculated for the Peroxides Using Parameter Set OPT9 (O–O = 1.49 Å)

	a (Å)	c (Å)	V (Å^3)	W (kJ mol^{-1})
SrO_2				
Lit.	3.568	6.616	84.23	−3050[a]
Calc.	3.565	6.621	84.15	−3113
% error	0.08%	−0.07%	0.10%	−2.1
BaO_2				
Lit.	3.807	6.841	99.15	−3000[a]
Calc.	3.823	6.821	99.69	−2718
% error	−0.40%	0.30%	−0.54%	9.4

[a] Lattice energies calculated by Vedeneev *et al.* (11).

TABLE 4
Comparison of Lattice Energies (kJ mol^{-1}) Reported for the Alkaline–Earth Metal Peroxides

Reference	CaO_2	SrO_2	BaO_2
Kapustinskii (12)	−3050	−2865	−2738
Therm. cycle[a]	−3133	−2849	—
1949: EU[b]	−3075	−2920	−2707
1952: V[c]	—	−3050	−3000
1965: WD[d]	−3144	−3037	—
1996: WMIN(OPT9)[e]	—	−3113	−2718

[a] Therm. cycle = lattice energy calculated from the thermochemical (Born-Haber) cycle (9).
[b] EU = Evans and Uri (13).
[c] V = Vedeneev *et al.* (11).
[d] WD = Wood and D'Orazio (14).
[e] WMIN (OPT9) = lattice energies calculated using OPT9.

Setting the Decomposition Pathway

The assumptions made in modeling the peroxide decomposition route were analogous to those for the carbonate decomposition route (1): (i) The reactants are pure crystalline peroxides (SrO_2 or BaO_2), tetragonal space group $I4/mmm$. (ii) The final solid products are the corresponding pure crystalline (Sr or Ba) oxides, cubic space group $Fm\bar{3}m$. (iii) Reaction is assumed to occur *via* a series of solid intermediates with structures changing along a symmetry route (see below) connecting $I4/mmm$ to $Fm\bar{3}m$. (iv) Parameters needed for calculating the lattice energies of intermediates are assumed to be transferable from the known structure to the intermediate of similar composition. Thus, for the intermediate structures, the parameter set for either the peroxides or the oxides, depending on whether the oxidation state of oxygen was −1 or −2, was used. (v) The crystal structures are assumed to be perfect; no allowance is made for the influence of any kind of defect on the lattice energy.

During the modeled overall decomposition, the peroxide ions, which are aligned parallel to the tetragonal c-axis, become converted to oxide ions and the tetragonal c-axis shrinks to its value in the cubic structure, with only relatively small changes in the a dimension (see Fig. 1, i.e., structure 1 → structure 3*).

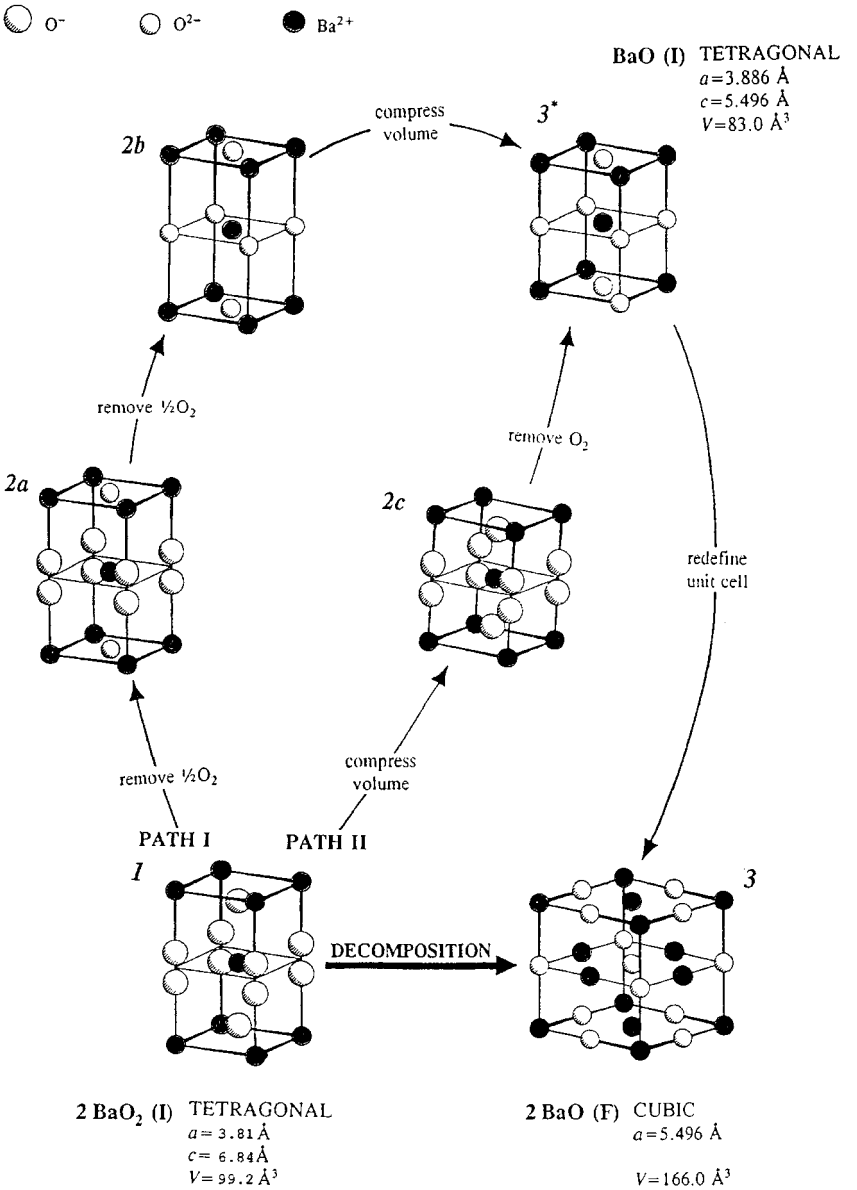

FIG. 1. Postulated symmetry-controlled transformations for the decomposition of BaO_2 to BaO.

Two symmetry-controlled transformations for the decomposition (see Fig. 1), starting from the reactant, structure 1 (tetragonal, body-centered unit cell with $a = 3.568$ Å, $c = 6.616$ Å for SrO_2; $a = 3.807$ Å, $c = 6.841$ Å for BaO_2 ($Z = 2$)), to the product, structure 3 (cubic, face-centered unit cell with $a = 5.1396$ Å for SrO, and $a = 5.496$ Å for BaO ($Z = 4$)) were investigated. To obtain structure 3 from structure 3*, the unit cell has to be redefined (without energy change) to convert the body-centered arrangement to a face-centered arrangement.

PATH I: removal of O_2 from the peroxide gives structure 2b, followed by adjustments to the unit cell dimensions to achieve those of the oxide structure.

PATH II: adjustment of the peroxide unit cell dimensions to those of the oxide, giving structure 2c. Since the positions of the atoms are recorded in fractional coordinates (and the coordinates of the peroxide ion (O^-–O^-) are $(0, 0, z)$ and $(0, 0, \bar{z})$), the z-coordinates of the O^- ions have to the corrected to keep the O–O bond length constant. Once the peroxide ion has been converted to the oxide ion, O^{2-}, with the removal of O_2(g) as in the next stage (i.e., structure 3*), this problem no longer exists.

(Note that Fig. 1 shows the O_2 being removed in stages in PATH I via the intermediate structure 2a. This sequence was only considered at a later stage and is discussed below).

After the trends in the changes of lattice energies along PATH I and PATH II were established, refinements to the crossover point between decreasing the volume of the unit cell and removing the O_2 were investigated, and the effects of these processes on the activation energy for the decomposition were determined. Since there are two O_2^{2-} ions per unit cell, the effect of removing one O_2^{2-} at a time was also explored.

In structure 2a (Fig. 1) oxygen is in a mixed oxidation state; thus there are three oxygen–oxygen interactions, O^{2-}–O^{2-}, O^{-}–O^{-} and O^{2-}–O^{-}. The energy parameters for the O^{2-}–O^{-} interactions were calculated from the geometric means (A_{ij},C_{ij}) and arithmetic means (ρ_{ij}) of the parameters for the oxides and peroxides. Corrections to the z-coordinates of the peroxide ion were made for all unit cell deformations in which the peroxide ion(s) were still present. The lattice energies calculated for PATH I and PATH II in the proposed decomposition route (see Fig. 1) are listed in Table 5. Only approximate calculations were done for structure 2a, and values obtained lay between those for structure 1 and structure 2b.

The decompositions of the alkaline–earth peroxides are endothermic (2). The enthalpy changes for the decompositions, calculated from standard enthalpies of formation (9), are 52.3 kJ mol^{-1} for SrO_2 and 71.6 kJ mol^{-1} for BaO_2. Values measured from DSC traces by Tribelhorn and Brown (2), i.e., 51.7 and 76.2 kJ mol^{-1}, compare favorably. To relate the changes in lattice energy to the changes in energy associated with the decomposition of the peroxides, corrections have to be made for the removal of O_2 from the lattice.

Correction for the Removal of O_2

From the definition of lattice energy, the processes under consideration are:

$$MO_2(s) \rightarrow M^{2+}(g) + O_2^{2-}(g) \quad \cdots \quad \Delta H_1 \qquad [1]$$

$$MO(s) \rightarrow M^{2+}(g) + O^{2-}(g) \quad \cdots \quad \Delta H_2. \qquad [2]$$

TABLE 5
Calculated Lattice Energies for Structures (Excluding Structure 2a) in the Proposed Symmetry-Controlled Routes in the Decompositions of the Alkaline–Earth Peroxides (see Fig. 1)

W (kJ mol^{-1})	SrO_2	BaO_2
PATH 1		
Structure 1	− 3113	− 2718
Structure 2b	− 3201	− 2993
Structure 3	− 3240	− 3020
PATH II		
Structure 1	− 3113	− 2718
Structure 2c	− 2802	− 2604
Structure 3	− 3240	− 3020

Lattice energies are formally calculated at 0 K, but crystal structure data refer to room temperature, so that fitting is effectively at room temperature. Now, $\Delta H = \Delta U + \rho\Delta V \approx \Delta U + \Delta n\mathrm{RT}$, where Δn (= 2 for reactions [1] and [2]) is the change in the number of gaseous molecules. Therefore, using $T = 298$ K, $\Delta n\mathrm{RT} \approx 5$ kJ mol^{-1}. This is within the uncertainties of the lattice energy values, and so $\Delta H \approx \Delta U = -W$ for the formation of gaseous ions.

For the reaction [1] − [2],

$$MO_2(s) \rightarrow MO(s) + O_2^{2-}(g) - O^{2-}(g) \quad \cdots$$

$$\Delta H_3 = \Delta H_1 - \Delta H_2. \qquad [3]$$

For decomposition,

$$MO_2(s) \rightarrow MO(s) + \tfrac{1}{2}O_2(g) \quad \cdots \quad \Delta H_4. \qquad [4]$$

ΔH_4 is calculated from tables of standard thermodynamic data (15).

Finally, [4] − [3] yields

$$O_2^{2-}(s) \rightarrow \tfrac{1}{2}O_2(g) + O^{2-}(g) \quad \cdots \quad \Delta H_5 = \Delta H_4 - \Delta H_3. \qquad [5]$$

Reaction [5] represents the reaction that takes place on removal of O_2 from the lattice and, therefore, the value of ΔH_5 must be added to those energies calculated from the lattice devoid of O_2. Table 6 gives the enthalpies for reactions [1] to [5] for Sr and Ba. The processes involved are summarized in Fig. 2.

Reaction Profiles

The energies corrected for the removal of O_2 from BaO_2 (see Table 7) are plotted against course of reaction in Fig. 3. The heights of the energy barriers in the corrected decomposition profiles were used to calculate apparent activation energies (E_a) (see Table 8). For the proposed decomposition

TABLE 6
Enthalpies of Reaction (in kJ mol^{-1}) of the Reactions Defined in the Text

	SrO_2	BaO_2
ΔH_1	3113	2718
ΔH_2	3240	3021
ΔH_3	− 127	− 303
ΔH_4	52	72
ΔH_5	179	374

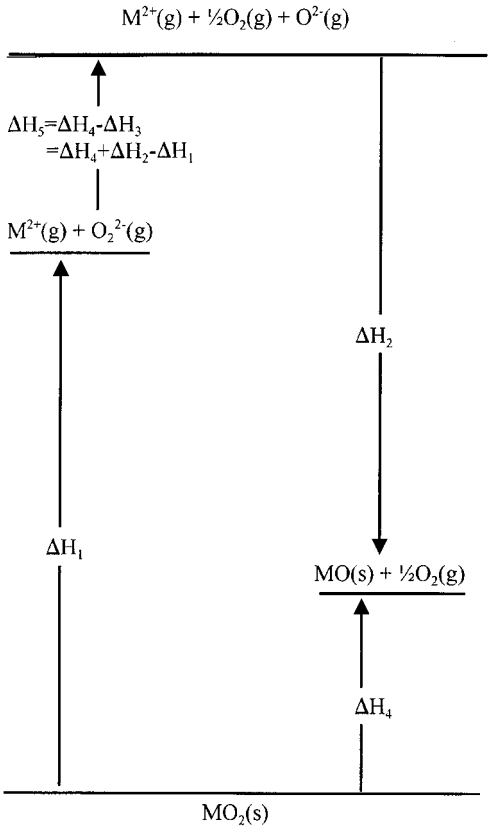

FIG. 2. The full energetic path: reactant to product via gaseous ions (not to scale).

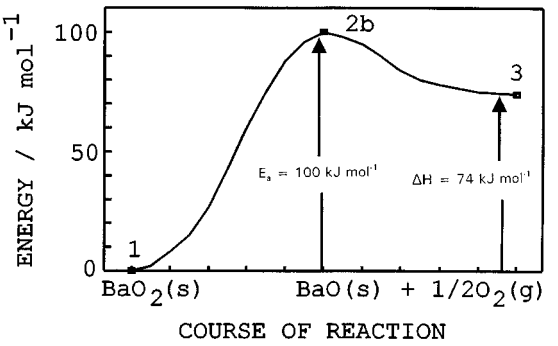

FIG. 3. Change in lattice energies (corrected for the removal of $\frac{1}{2}O_2$) with reference to the lattice energy of BaO_2, plotted against the course of the decomposition of BaO_2. Structure numbers indicated are from Table 5.

route (PATH I), E_a was calculated to be 91 and 99 kJ mol^{-1} for SrO_2 and BaO_2, respectively.

The activation energies calculated from PATH II were considerably higher for SrO_2 and in the reverse order, i.e., 311 and 114 kJ mol^{-1} for SrO_2 and BaO_2, respectively.

TABLE 7
Calculated Lattice Energies for Structures (Excluding Structure 2a) in the Proposed Symmetry-Controlled Routes for the decomposition of Barium Peroxide

	W (kJ mol^{-1})	$W_{corrected}$ (kJ mol^{-1})	ΔW_1 (kJ mol^{-1})
PATH I			
Structure 1	− 2718	− 2718	0
Structure 2b	− 2993	− 2619	99
Structure 3	− 3020	− 2646	72

Notes. $W_{corrected} = W$ corrected for the removal of O_2 and $\Delta W_1 =$ change in corrected energies with respect to structure 1 (BaO_2). $W_{corrected} = W - \Delta H_5 = W - 374$ kJ mol^{-1}.

DISCUSSION AND CONCLUSIONS

The activation energies predicted for the decomposition of SrO_2 (91 kJ mol^{-1}) and BaO_2 (99 kJ mol^{-1}) are lower than experimental (2,17,18) values (for example, 119 and 185 kJ mol^{-1} for Sr and Ba, respectively (2)). The predicted activation energies, however, follow the expected trend: as the lattice energy decreases (i.e., down the group, $Ca^{2+} \rightarrow Ba^{2+}$), the activation energy increases.

All oxygen positions in the peroxide lattice (for both Sr and Ba) are identical and therefore the removal of one oxygen is not favored over another. However, approximate calculations based on structure 2a show that the lattice energy increases on removal of the first oxygen atom from the unit cell, and then increases further with removal of the second oxygen atom, so that the maximum energy barrier is associated with the removal of both oxygen atoms from the unit cell.

Several studies of the decomposition of the alkaline–earth metal peroxides have been reported (2). It is clear that the thermal decomposition is more complicated than the simple process represented by $MO_2(s) \rightarrow MO(s) + \frac{1}{2}O_2(g)$. Only a few of these studies report values for the kinetic parameters. E_a values for SrO_2 (119 to 165 kJ mol^{-1}) and BaO_2

TABLE 8
Activation Energies (kJ mol^{-1}) for the Decompositions of Sr and Ba Peroxides

	BaO_2		SrO_2	
Reference	Isothermal	Non-iso	Isothermal	Non-iso
(17)	192	360 ± 20	—	—
(18)	135	141	—	—
(2)	185	165	119	165
This study	99		91	

(135 to 360 kJ mol^{-1}), calculated from both isothermal and nonisothermal kinetic studies, are shown in Table 8. Brunere *et al.* (16) represented the decomposition of BaO_2 by a three-step process: nucleus formation (E_a = 12 kJ mol^{-1}), grain growth (E_a = 104 kJ mol^{-1}), and oxygen diffusion (E_a = 2 kJ mol^{-1}).

The decompositions of the peroxides are known to be reversible and, in the lattice energy calculations, no account can be taken of any influence of the reverse process, which may be considerable when removal of product oxygen gas is not rapid or complete. Ideally then, the values from lattice energy calculations should be closest to experimental values obtained for the decomposition of the peroxides in vacuum.

When different mechanisms operate over different temperature ranges, an explanation for a change of mechanism could be the influence of some recrystallization of the product oxide on the course of reaction, i.e.,

$$MO_2(s) \rightarrow MO(a) + \tfrac{1}{2}O_2(g)$$

$$MO(a) \rightarrow MO(c),$$

where c = crystalline and a = amorphous. Such processes have been suggested in the dehydration of hydrates and in many decompositions, especially those of the alkaline–earth metal carbonates. The rate of removal of oxygen from the peroxide by diffusion could be drastically altered by the formation of a crystalline layer of oxide on the surface from which O_2 gas is eventually to be released.

Kinetic Implications

The calculated energy barriers for the postulated highly symmetry-controlled reaction routes of the peroxides are lower than the experimental values. The opposite would be expected (and has been found for the carbonates examined in Part 1), since the realistic, defect-mediated processes would be expected to be less energy-demanding than the stylized route chosen here.

Unexpectedly low activation energies can be interpreted to mean that the chosen route is energetically inaccessible to the decomposition, i.e., the breakdown of O_2^{2-} to O^{2-} with release of O_2 requires steps (such as destruction of the crystal structure) which are energetically prohibitive, and so the direct process cannot be followed. Consequently, the decomposition must follow a more tortuous, if less energy-demanding, path. Other barriers to the processes of decomposition and lattice reconstruction may include a chemical activation barrier to the conversion of peroxide to oxide ion or kinetic barriers to the escape of the released O_2, requiring disruption of the lattice in some fashion.

This interesting result suggests that the procedure adopted here of following the energetics of a decomposition via a postulated path may be used to direct attention away from impracticable decomposition routes and allow exploration of more feasible mechanisms.

REFERENCES

1. A. de La Croix, R. B. English, M. E. Brown, and L. Glasser, *J. Solid State Chem.* **137,** 332 (1998).
2. M. J. Tribelhorn and M. E. Brown, *Thermochim. Acta* **225,** 143 (1995).
3. W. R. Busing, "WMIN: A computer program to model molecules and crystals in terms of potential energy functions," ORNL-5747. U.S., Oak Ridge National Laboratory, 1981. Revised version, March 1994.
4. S. C. Abrahams and J. Kalnajs, *Acta Crystallogr.* **7,** 838 (1954).
5. V. Kotov and S. Reichstein, *Zh. Fiz. Khim.* **15,** 1057 (1941); *Chem. Abstr.* **36,** 5073.
6. J. D. Bernal, E. Djatlowa, P. Kasarnwsky, S. Reichstein, and A. G. Ward, *Z. Kristallogr.* **92,** 344 (1935); *Chem. Abstr.* **30,** 2821.
7. C. Brosset and N. G. Vannerberg, *Nature* (*London*) **177,** 238 (1956).
8. J. V. Smith, "Powder Diffraction File," No. 7-234, 1956.
9. R. C. Weast, Chief Ed., "Handbook of Chemistry and Physics," 64th ed. CRC Press, Florida, 1983.
10. S. I. Raikhstiin and I. Kazarnovskii, *Zh. Fiz. Khim.* **3,** 83 (1932); *Chem. Abstr.* **27,** 676.
11. A. V. Vedeneev, L. I. Kazarnovskaya, and I. A. Kazarnovskii, *Zh. Fiz. Khim.* **26,** 1808 (1952); *Chem. Abstr.* **47,** 5786.
12. A. F. Kapustinskii, *Z. Phys. Chem.* (*Leipzig*) **B22,** 257 (1933); *Chem. Abstr.* **27,** 5227; *J. Phys. Chem.* (*USSR*) **5,** 59 (1934); *Chem. Abstr.* **28,** 4955; *Acta Physicochim. URSS* **18,** 370 (1943); *Chem. Abstr.* **38,** 5705.
13. M. G. Evans and N. Uri, *Trans. Faraday Soc.* **45,** 224 (1949).
14. R. H. Wood and L. A. D'Orazio, *J. Phys. Chem.* **69,** 2558 (1965).
15. F. D. Rossini, D. D. Wagman, W. H. Evans, S. Levine, and I. Jaffe (Eds.), "Selected Values of Chemical Thermodynamic Properties," Circular of the National Bureau of Standards 500. United States Government Printing Office, Washington, DC, 1952.
16. V. J. Brunere and A. N. Dokuchaeva, *Izv. Akad. Nauk. Latvijskoj SSR, Ser. Chim.* **3,** 332 (1990); *Chem. Abstr.* **113,** 104146v.
17. B. J. Erofeev and N. D. Sokolova, *Akad. Nauk BSSR Minsk* **3** (1963); *Chem. Abstr.* **62,** 3434a, quoted in A. F. Mayorova, S. N. Mudretsova, M. N. Mamontov, P. A. Levashov, and A. D. Rushin, *Thermochim. Acta* **217,** 241 (1993).
18. M. A. Fahim and J. D. Ford, *J. Chem. Eng.* **27,** 21 (1983).